Reconstitution of Membrane Proteins into Polymer-Supported Membranes for Probing Diffusion and Interactions by Single Molecule Techniques

ARTICLE *in* ANALYTICAL CHEMISTRY · AUGUST 2011

Impact Factor: 5.64 · DOI: 10.1021/ac201294v · Source: PubMed

7 AUTHORS, INCLUDING:

Robin Schubert
University of Hamburg
5 PUBLICATIONS **19** CITATIONS
SEE PROFILE

Christian Paolo Richter
Universität Osnabrück
16 PUBLICATIONS **192** CITATIONS
SEE PROFILE

Bo Liedberg
Nanyang Technological University
270 PUBLICATIONS **9,845** CITATIONS
SEE PROFILE

Jacob Piehler
Universität Osnabrück
158 PUBLICATIONS **4,959** CITATIONS
SEE PROFILE

analytical chemistry

ARTICLE

pubs.acs.org/ac

Reconstitution of Membrane Proteins into Polymer-Supported Membranes for Probing Diffusion and Interactions by Single Molecule Techniques

Friedrich Roder,[†] Sharon Waichman,[†,‡] Dirk Paterok,[†] Robin Schubert,[†] Christian Richter,[†] Bo Liedberg,[‡] and Jacob Piehler*[,†]

[†]Division of Biophysics, University of Osnabrück, Germany

[‡]Division of Molecular Physics, Linköping University, Sweden

Supporting Information

ABSTRACT: We have established a robust and versatile analytical platform for probing membrane protein function in a defined lipid environment on solid supports. This approach is based on vesicle capturing onto an ultrathin poly(ethylene glycol) (PEG) polymer brush functionalized with fatty acid moieties and subsequent vesicle fusion into a contiguous membrane. In order to ensure efficient formation of these tethered polymer-supported membranes (PSM), very small unilamellar vesicles (VSUV) containing fluorescent lipids or model transmembrane proteins were generated by detergent depletion with cyclodextrin. Thus, very rapid reconstitution of membrane proteins into PSM was possible in a format compatible with microfluidics. Moreover, surfaces could be regenerated with detergent solution and reused multiple times. Lipid and protein diffusion in these membranes was investigated by fluorescence recovery after photobleaching, single molecule tracking, and fluorescence correlation spectroscopy. Full mobility of lipids and a high degree of protein mobility as well as homogeneous diffusion of both were observed. Quantitative ligand binding studies by solid phase detection techniques confirmed functional integrity of a transmembrane receptor reconstituted into these PSM. Colocomotion of individual ligand−receptor complexes was detected, demonstrating the applicability for single molecule fluorescence techniques.

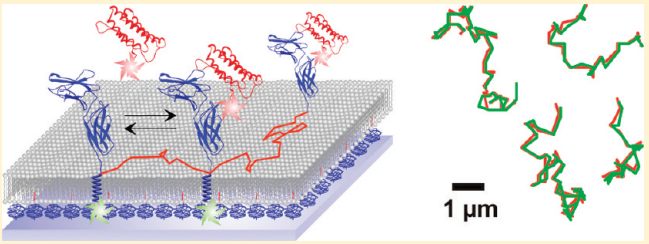

Functional analysis of isolated membrane proteins in vitro requires reconstitution into lipid membranes, as the conformations and the functions of these proteins often critically depend on the lipid environment.[1−6] In order to cope with the low abundance and stability of most membrane proteins, efficient analytical platforms are required for rapid and efficient reconstitution, which are compatible with a broad range of spectroscopic techniques. In particular, single molecule fluorescence techniques offer versatile means to investigate the complex interplay between the dynamics of diffusion within the membrane and the interactions with soluble and membranous interaction partners as well as potential conformational changes.[7−11] Solid-supported membranes are readily combined with a broad range of spectroscopic and microscopic techniques[12−17] and are readily combined with microfluidics for versatile and multiplexed sample handling.[18,19] For reconstitution of transmembrane proteins, thin polymer cushions are required in order to minimize nonspecific interactions with the substrate surface.[12,20−23] Such polymer-supported membranes (PSM) have been successfully used to reconstitute transmembrane proteins on different substrates.[20−22,24−29] Commonly, the substrates are coated with ultrathin layers of hydrophilic, noncharged polymers such as carbohydrates or poly(ethylene glycol) (PEG). Typically, these polymers do not interact with lipids or liposomes and spontaneous vesicle fusion is not observed except on very rigid polysaccharide layers.[30] For more efficient vesicle capturing and membrane tethering, hydrophobic anchoring groups are incorporated.[31] Membrane protein reconstitution into PSM has been achieved by using tethered lipid monolayer assembly based on Langmuir−Blodgett transfer,[25,32,33] which is rather intricate and time-consuming. For analytical applications requiring flow-through sample handling, repeated use of the same substrate surface for membrane protein reconstitution in PSM is desired, which is not possible by this approach. Thus, self-assembly of PSM via vesicle fusion initiated by covalently attached hydrophobic anchoring groups are more suitable for high-throughput application.[34,35] This approach also provides versatile means for lateral organization of membranes in micropatterns,[35−37] which is an important prerequisite for multiplexed assays. However, obtaining contiguous and homogeneous PSM by direct vesicle fusion is challenging. At high densities of hydrophobic anchoring groups required for efficient vesicle

Received: June 13, 2011
Accepted: July 19, 2011
Published: August 12, 2011

Scheme 1. Strategy for Protein Reconstitution in Polymer-Supported Membranes[a]

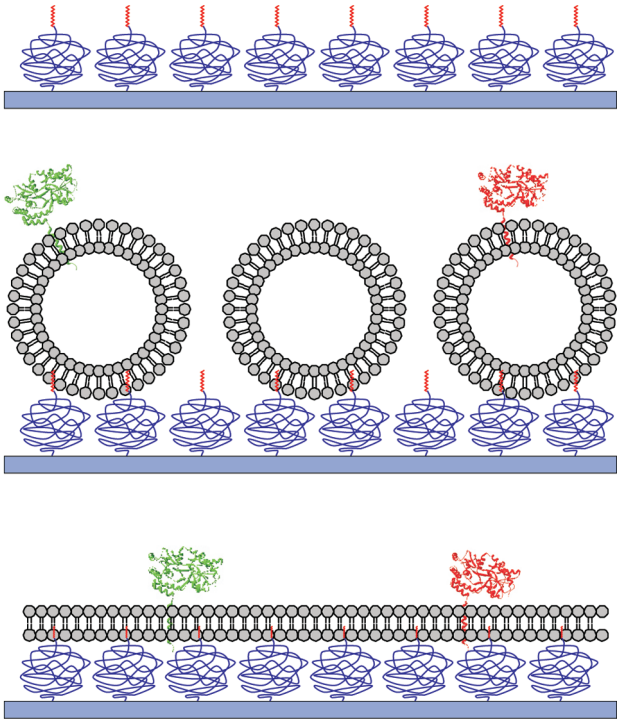

[a] Schematic of the surface architecture (top), (proteo)liposome binding to the surface (center), and fusion of the vesicles to form an extended polymer-supported membrane (bottom).

fusion, free diffusion of proteins is obstructed.[33] At low density, however, hydrophobic anchoring groups do not effectively initiate vesicle fusion but merely yield tethered vesicles.[34,38]

Here, we have implemented a versatile approach for membrane protein reconstitution in polymer-supported membranes which is compatible with many ensemble and single molecule detection techniques as well as fluidic sample handling. This approach is based on membrane protein reconstitution into highly monodisperse very small unilamellar vesicles (VSUV), which were generated by detergent extraction with cyclodextrin.[39] We demonstrate that liposomes and proteoliposomes obtained by this technique are readily fused after capturing to a PEG polymer brush functionalized with palmitic acid groups (Scheme 1). We show fast and homogeneous diffusion of lipids and model transmembrane proteins within these membranes using fluorescence recovery after photobleaching (FRAP), fluorescence correlation spectroscopy (FCS), and single molecule tracking (SMT). This approach was successfully employed for probing diffusion and ligand interactions of the transmembrane type I interferon (IFN) receptor subunit IFNAR2 by SMT and total internal reflection fluorescence spectroscopy (TIRFS).

EXPERIMENTAL SECTION

Materials. Materials and experimental procedures for protein production and labeling are described in the Supporting Information. Surface Chemistry and Surface CharacterizationSurface chemistry was carried out on natively oxidized silicon wafers, on transducer slides for reflectance interference detection (a thin silica layer on a glass substrate), and on glass cover slides for fluorescence microscopy. Surface coating with a thin PEG polymer brush and further functionalization was carried out as described in detail previously:[40] After surface cleaning in fresh piranha solution (one part H_2O_2 30% and two parts concentrated H_2SO_4) the surface was activated by reaction with pure GOPTS for 1 h at 75 °C. Subsequently, the surface was reacted with molten DAPEG for 4 h at 75 °C. Thereafter, a solution of 0.5 M palmitic acid and di-isopropylcarbodiimide in DMSO was incubated for 45 min at room temperature. Surface characterization by ellipsometry and contact dynamic angle goniometry is described in the Supporting Information.

Preparation of Liposomes and Proteoliposomes. Liposomes and proteoliposomes were prepared from detergent solution by addition of cyclodextrin which was described previously.[39] A thin lipid film was prepared from a solution of SOPC in chloroform, which was removed in vacuo. This lipid film was solubilized in 20 mM Hepes, 150 mM NaCl, pH 7,4 (HBS) supplemented with Triton X-100 resulting in a lipid-detergent stock solution of 5 mM SOPC and 20 mM Triton X-100. Liposomes were prepared from a 20-fold dilution of the stock solution in HBS by addition of cyclodextrin to a concentration of 2 mM followed by thorough mixing. Incorporation of the fluorescent lipids BHPC, OG-DHPE, or DiD into the vesicles was achieved by preparation of lipid-detergent stock solutions with molar ratios for fluorescent lipid/SOPC of $1{:}10^3$ for an ensemble and $1{:}10^{6-7}$ for single molecule measurements. Reconstitution of transmembrane proteins was achieved by incubation of the lipid-detergent stock solution with the protein for >10 min, 20-fold dilution in HBS containing 25 mM EDTA (HBSE), and subsequent detergent removal by cyclodextrin. The fluorescently labeled transmembrane proteins were added in molar ratios of $1{:}10^3$ (labeled protein/SOPC) for ensemble measurements. Ratios of $1{:}10^{6-7}$ (labeled protein/SOPC) were used for FCS and SMT. The protein reconstitution samples for single molecule studies contained additional unlabeled MBP-ALA_7 at a ratio of $1{:}10^3$ (protein/SOPC) in order to minimize unspecific interactions of labeled protein with the surface.

Quantitative Analysis of Diffusion and Interaction. Vesicle binding and fusion at surfaces, protein reconstitution, and protein−protein interactions were monitored in real time by simultaneous TIRFS and reflectance interference (RIF) detection in a flow-through system using a home-built setup, which has been described before.[41,42] All experiments were carried out in HBSE. Diffusion of fluorescence-labeled lipids and proteins was explored by FRAP, SMT, and FCS as described in detail in the Supporting Information.

RESULTS AND DISCUSSION

Surface Modification. For selective capturing of liposomes onto the surface of a dense polymer cushion, we coupled palmitic acid moieties to an amine-functionalized PEG polymer brush (PEG/PA). Ellipsometric analysis of the surface layer confirmed a high-density PEG layer. Approximately 60% of the PEG chains were reacted with palmitic acid (Supporting Table S-1 in the Supporting Information) yielding a density of 0.5 palmitic acid moieties per nm^2. Dynamic contact angle measurements revealed that the functionalization of the PEG polymer brush with palmitic acid moieties was accompanied by a significant increase in the hydrophobicity (Supporting Table S-1 in the Supporting Information). However, this increase in hydrophobicity was moderate compared to a silanized surface directly modified with

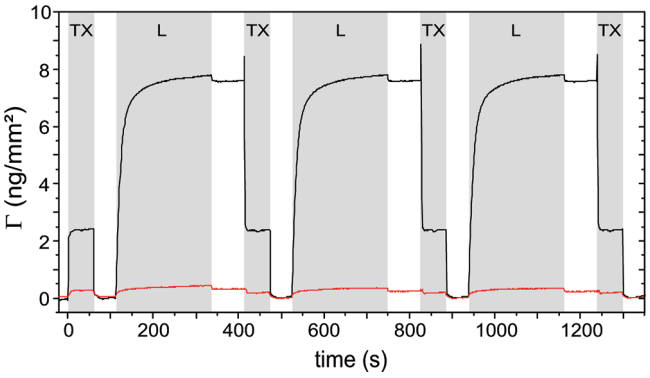

Figure 1. Liposome binding on a PEG polymer brush explored by label-free detection. Repeated binding of VSUV (L) to a PEG polymer brush functionalized with palmitic acid followed by regeneration with detergent solution (TX) (black curve). For comparison, binding of VSUV to a nonfunctionalized PEG polymer brush is shown (red curve).

hexadecane thiol (Θ_a, 93°; Θ_r, 64°).[40] Thus, a relatively high density of anchoring groups was achieved without rendering the surface extremely hydrophobic.

Vesicle Capturing with Hydrophobic Anchoring Groups. All reconstitution experiments were carried out with pure SOPC, which guarantees membrane fluidity at room temperature and an electrostatically neutral membrane surface. For the preparation of small unilaminar vesicles (SUV) and proteoliposomes, we employed rapid detergent depletion by cyclodextrin that forms an inclusion complex with the detergent.[39,43] Surprisingly, the SUV obtained by this method were so small, that very little light scattering was observed in the solution. We therefore characterized the size distribution in more detail by dynamic light scattering and by transmission electron microscopy (Figure S-1 in the Supporting Information). These measurements confirmed the formation of very small unilaminar vesicles (VSUV) and proteoliposomes with an average diameter of 18−25 nm and a narrow size distribution. Capturing these VSUV to PEG polymer brush-modified surfaces functionalized with palmitic acid moieties was quantitatively probed by label-free detection using reflectance interference detection (RIF). Upon injection of VSUV, strong binding was observed (Figure 1) reaching a typical surface loading of 7−8 ng/mm^2. A lipid bilayer obtained by vesicle fusion on a clean glass support yields only 4−5 ng/mm^2. Vesicles could be removed quantitatively by injection of detergent, and the same binding signal was obtained upon subsequent injection of VSUV (Figure 1). Reversible vesicle capturing was possible on the same surface for dozens of cycles without a significant loss in binding capacity. Specific vesicle capturing by palmitic acid anchoring groups was confirmed by negative control experiments with nonfunctionalized PEG surfaces (Figure 1).

PEG-Induced Vesicle Fusion. After capturing VSUV containing a lipid analogue labeled with BODIPY-FL (BHPC) onto palmitic acid-functionalized surfaces, a homogeneous fluorescence distribution on the surface was observed by confocal fluorescence microscopy (Figure S-2 in the Supporting Information). Upon bleaching of a circular spot, insignificant FRAP was observed, suggesting that the vesicles remained intact on the polymer cushion (Figure S-2 in the Supporting Information). Vesicle fusion was induced by incubation with a 10% PEG solution (7000−9000 g/mol),[34,44] yielding membrane inhomogeneities, which were efficiently removed by strong washing with buffer at a flow rate of 100−200 μL/s (Figure S-2 in the Supporting Information). FRAP experiments confirmed high lipid mobility after this treatment (Figure S-2 in the Supporting Information), suggesting efficient fusion of captured vesicles on the surface. Fast kinetics of PEG-induced vesicle fusion on the surface was corroborated by simultaneous TIRFS-RIF detection using a mixture of VSUV loaded with high concentrations of lipids conjugated to FRET donor and acceptor dyes (Figure S-3 in the Supporting Information). Lipid diffusion kinetics in the resulting membranes was quantitatively explored by FRAP at different bleaching spot diameters. Under all conditions, rapid FRAP was observed with a mobile fraction close to 100%, confirming full fusion of captured liposomes. The diffusion times at different bleaching radii were determined by fitting the FRAP curves (Figure 2a). Very good linear correlation of the diffusion times with the bleaching radii confirmed homogeneous diffusion properties within the PSM (Figure 2b). A diffusion constant of 3.1 ± 0.4 μm^2/s was obtained for the BHPC probe. This diffusion constant is comparable to the mobility of lipids in PSM obtained by FRAP on ultrathin cellulose[45] and slightly higher than in PSM obtained by vesicle fusion onto the LB-transferred lipid monolayer.[25] Strikingly, a significantly higher mobile fraction of lipids was observed (∼100%) compared to these more sophisticated approaches. The PSM was quantitatively removed during washing with detergent, and fresh VSUV could be captured and fused again into a contiguous PSM. Throughout more than 10 repeated vesicle fusion experiments on the same surface, there were no significant changes in the diffusion properties of the lipid probes.

Lipid Mobility Explored by Single Molecule Techniques. In order to explore the local lipid mobility in the PSM, diffusion of the BHPC probe was probed by SMT. Rapid diffusion of individual BHPC was observed (Video 1 and Figure S-4 in the Supporting Information). The mobile fraction of lipids in the membrane could not be reliably analyzed by this method because of photobleaching, which eliminated the contribution by immobile molecules over time. Statistical analysis of the displacements after different lag times revealed highly monodisperse diffusion (Figure 2c), yielding a diffusion constant of 4.5 ± 0.5 μm^2/s (see Table 1). The strictly linear correlation of the mean square displacements with the lag time confirmed free Brownian diffusion (Figure 2d). Moreover, the local mobility of BHPC was measured using z-scan FCS that varies the observation area according to the focusing properties of the excitation laser light along the z-axis.[46,47] Typical autocorrelation curves obtained at different z-positions are shown in Figure S-4 in the Supporting Information, which were fitted well by a model considering a single species diffusing in two dimensions. From the diffusion times obtained at different z-positions (Figure 2e), an average diffusion constant of 5.9 ± 0.8 μm^2/s was determined. The linear correlation of the diffusion times with the squared beam radius has an intercept close to zero confirming free diffusion of the lipid probe (Figure 2f). This diffusion constant is close to the diffusion constants observed in giant unilaminar vesicles (GUV) demonstrating successful decoupling from the glass support.[48,49] Differences of the measured diffusion constants with different methods may be attributed to weak surface or tether interactions and would therefore depend on the detection area, which are very different for the different techniques (<1 μm^2 for z-scan FCS, ∼10 μm^2 for SMT, and 10−100 μm^2 for FRAP). However, even for highly homogeneous lipid membranes obtained by SUV fusion on glass support, similar differences in the diffusion

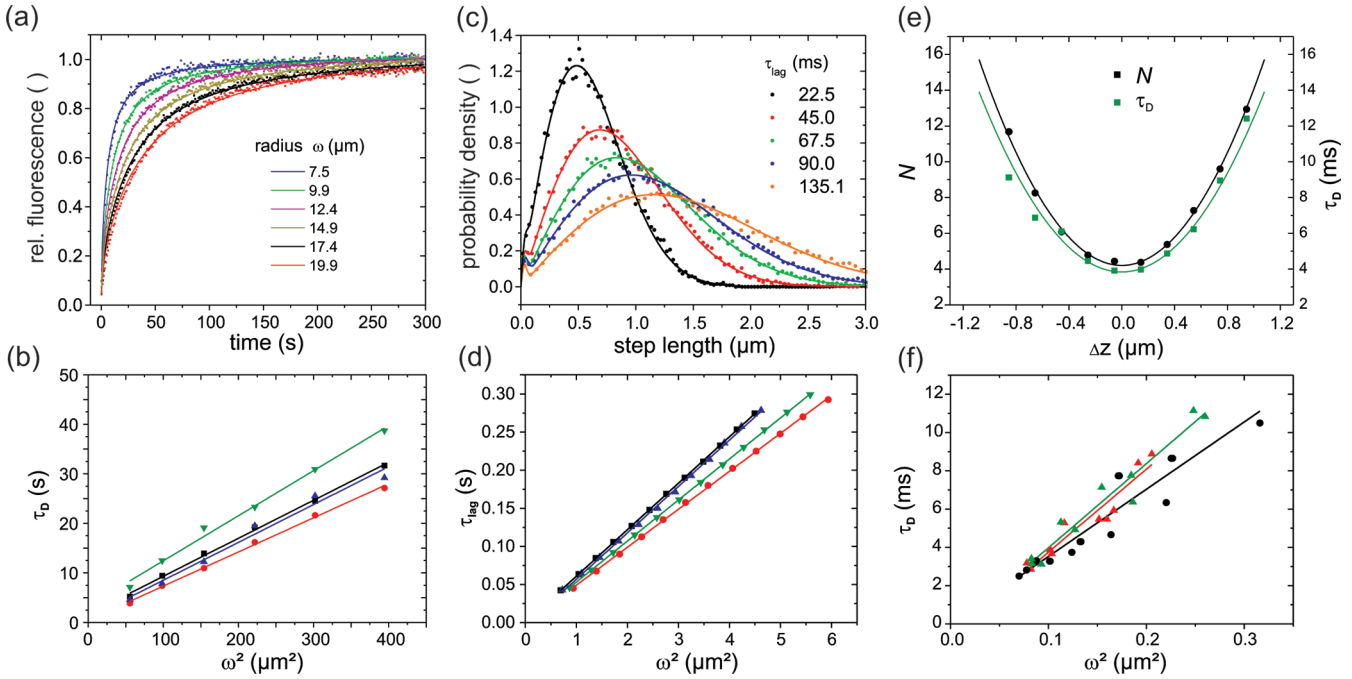

Figure 2. Lipid diffusion in PSM probed by FRAP (a, b), SMT (c, d), and FCS (e, f). (a) FRAP kinetics at different radii of the bleached spot and fit according to Soumpasis. (b) Diffusion times as a function of the squared radius of the bleached spot obtained on different surfaces. (c) Step-distance distribution analysis for different lag times (indicated in the legend). (d) Lag time τ as a function of the mean square displacements ω^2 obtained on different surfaces. (e) Diffusion times τ_D and number of particles in the confocal volume N as a function of the axial position of the confocal volume. (f) Diffusion time τ_D as a function of the squared beam radius ω^2 at the cross-section with the membrane obtained on different surfaces.

Table 1. Diffusion Constants of Lipid and Proteins Reconstituted into PSM

	D_{FRAP} [$\mu m^2/s$][a]	R_F [%][b]	D_{SMT} [$\mu m^2/s$][c]	D_{FCS} [$\mu m^2/s$][d]
lipid	3.08 ± 0.36	102 ± 3	4.46 ± 0.45	5.94 ± 0.81
MBP-TM1	0.52 ± 0.11	81 ± 2	0.74 ± 0.08	2.14 ± 0.49
IFNAR2-TM			0.64 ± 0.06	1.78 ± 0.46

[a] Diffusion constant from FRAP experiments. [b] Mobile fraction from FRAP experiments. [c] Diffusion constant from SMT experiments. [d] Diffusion constant from FCS experiments.

constants were observed.[49] Overall, our results confirmed free and homogeneous mobility of the lipid probe in the PSM from the nanometer to micrometer scale and the compatibility of the surface architecture with single molecule fluorescence techniques.

Protein Reconstitution into PSM. In the next step, we established reconstitution of model transmembrane proteins into these PSM. Proteoliposomes containing maltose binding protein fused to the transmembrane helix of IFNAR1 (MBP-TM1) labeled with Alexa Fluor 488 (^{AF488}MBP-TM1) were prepared by detergent extraction with cyclodextrin in exactly the same way as pure lipid VSUV. Orientation assays by proteinase K digestion suggested that ~80% of MBP-TM1 was oriented with the soluble MBP domain outside of the vesicle (Figure S-5 in the Supporting Information). Capturing of these VSUV to PEG surfaces functionalized with palmitic acid was monitored by simultaneous TIRFS-RIF detection (Figure S-6 in the Supporting Information). Similar kinetics and surface loadings for VSUV with and without proteins were observed by RIF. The fluorescence signals confirmed the efficient incorporation of MBP-TM1 into these VSUV. Full regeneration of the surface was observed upon injection of detergent solution, and very similar VSUV binding levels after regeneration confirmed the possibility for multiple experiments on the same surface. Nonreconstituted protein at the same effective concentration in detergent solution barely immobilized onto the surface demonstrating the selectivity of the surface for capturing vesicles. Formation of PSM from captured proteoliposomes and protein diffusion in PSM was explored by ensemble and single molecule imaging techniques. Confocal fluorescence imaging confirmed homogeneous distributions of proteoliposomes on the surface. After vesicle fusion with PEG and strong washing with buffer, homogeneous distribution and high FRAP was observed (Figure 3a). From quantitative analysis of the FRAP curves at different bleaching areas (Figure 3b), diffusion times were obtained, which showed a linear correlation to the square radius of the bleached area (Figure 3b). From these analyses, an average diffusion constant of 0.5 ± 0.1 $\mu m^2/s$ and a mobile fraction of 81 ± 2% were obtained for this protein. This diffusion constant is in very good agreement to the diffusion constant observed for similar membrane proteins on cellulose-supported membranes[45] and PEG-supported membranes produced by LB.[26]

Diffusion of Proteins in PSM Probed by SMT and FCS. We investigated the diffusion of individual transmembrane proteins reconstituted into PSM by SMT. For this purpose, ^{AF488}MBP-TM1 was reconstituted into liposomes at a very low protein/lipid ratio (1:10^6). In order to minimize nonspecific binding, unlabeled MBP-ALA_7 was coreconstituted at a higher protein/lipid ratio (1:10^3). These vesicles were fused on the solid support and the diffusion of individual proteins in the membrane could be observed by single molecule imaging (Video 2 in the Supporting Information). Typical trajectories are shown in Figure 4a. Trajectory analysis revealed homogeneous diffusion with a diffusion

dx.doi.org/10.1021/ac201294v |Anal. Chem. 2011, 83, 6792–6799

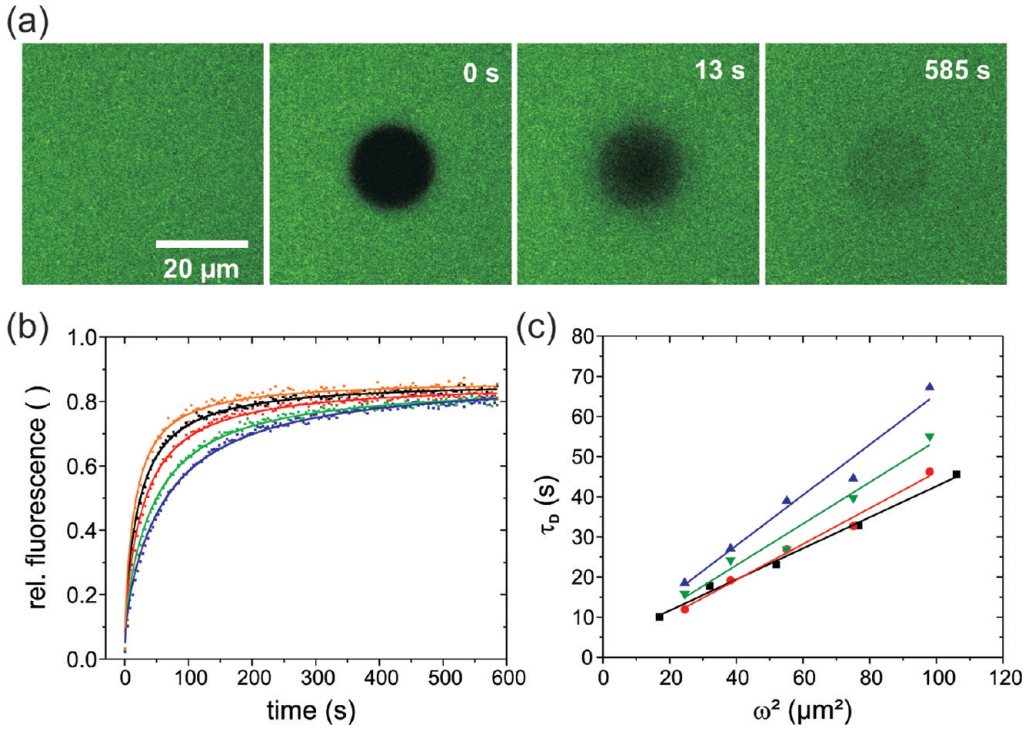

Figure 3. Diffusion of transmembrane proteins reconstituted in polymer-supported membranes: (a) typical FRAP experiment with reconstituted ^{AF488}MBP-TM1, (b) FRAP curves at different bleaching spots, and (c) diffusion time τ_D as a function of the bleaching area ω^2 for PSM obtained on different surfaces.

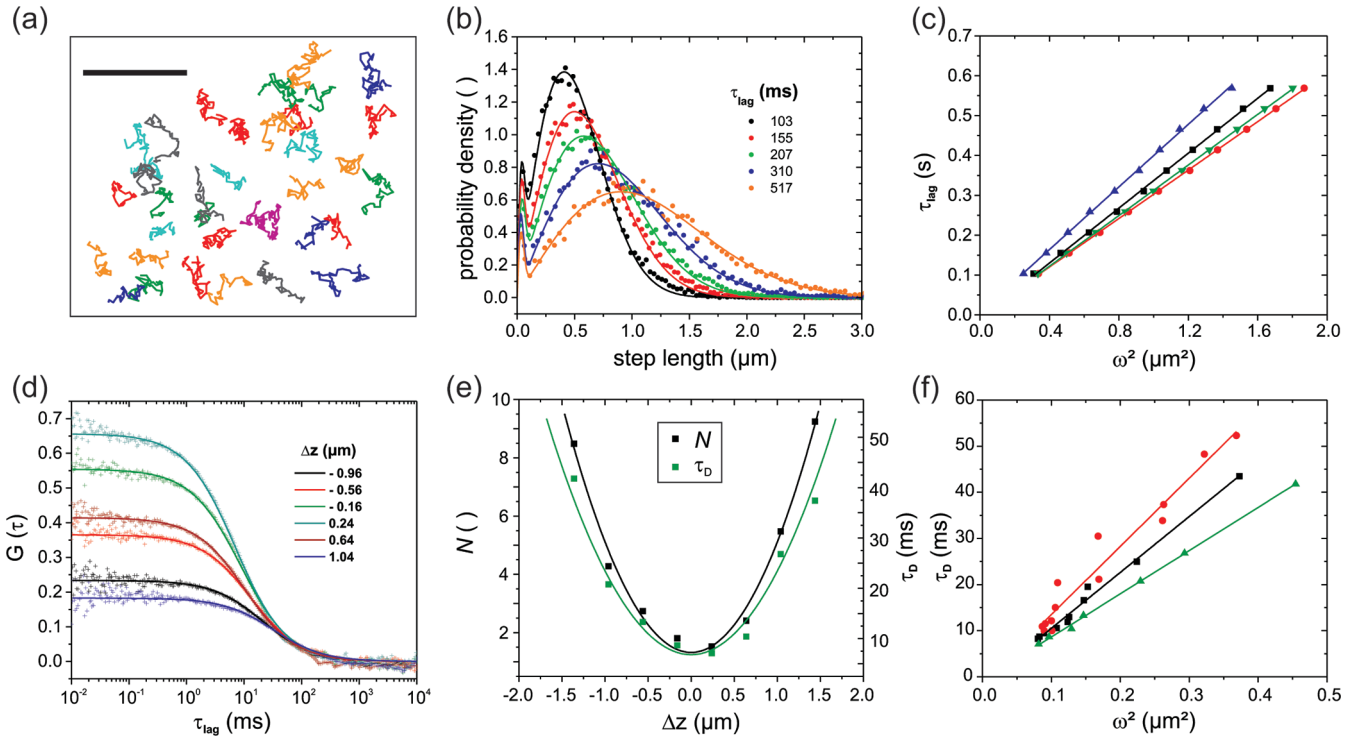

Figure 4. Membrane protein diffusion in PSM probed by SMT (a–c) and by z-scan FCS (d–f). (a) Trajectories obtained from imaging individual ^{AF488}MBP-TM1 molecules. The scale bar corresponds to 10 μm. (b) Displacement distribution analysis for different lag times. (c) Diffusion time as a function of the square displacement obtained on different surfaces. (d) Typical autocorrelation curves at different z-positions. (e) Diffusion times τ_D and average number of molecules in the confocal volume N as a function of the z-position. (f) Diffusion times τ_D as a function of the squared beam radius ω^2 at the cross-section with the membrane obtained on different surfaces.

dx.doi.org/10.1021/ac201294v |*Anal. Chem.* 2011, 83, 6792–6799

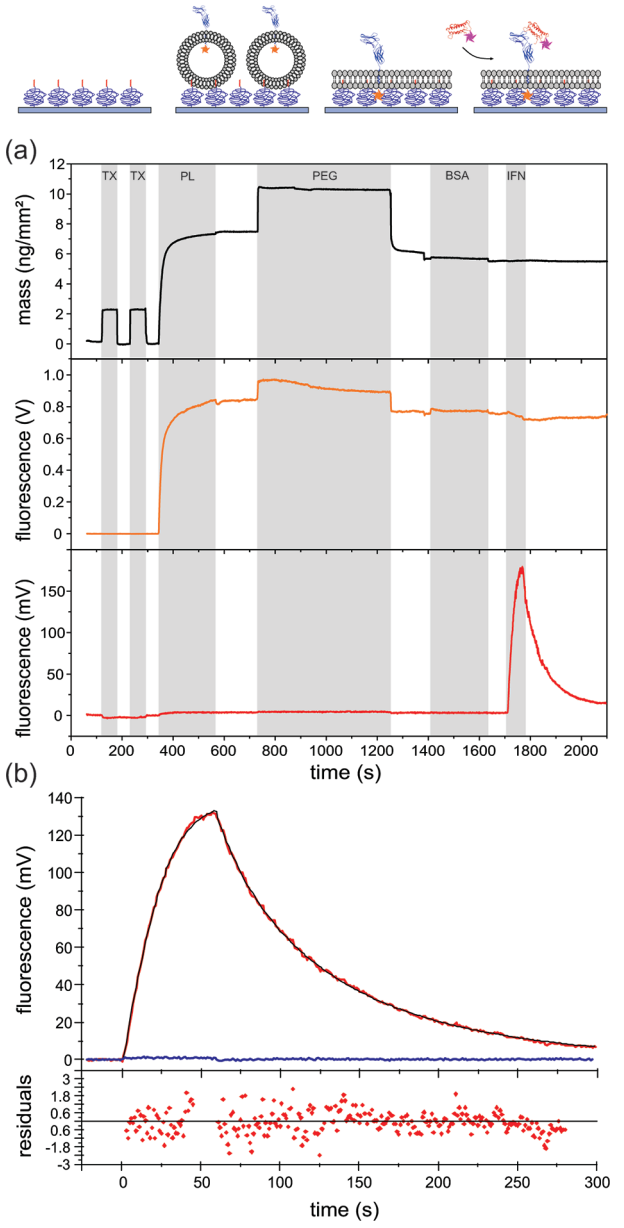

Figure 5. Specific ligand binding of a transmembrane receptor reconstituted into polymer-supported membranes. (a) Reconstitution of ^{Dy547}IFNAR2-TM into PSM as detected by simultaneous TIRFS-RIF detection. Top, RIF channel; center, yellow fluorescence (^{Dy547}IFNAR2-TM); bottom, red fluorescence (^{Dy647}IFNα2). After surface conditioning with Triton X-100 (TX), IFNAR2-TM reconstituted into proteoliposomes (PL) was injected, followed by fusion with PEG solution (PEG) and a strong wash. A BSA solution was injected to block unspecific binding (BSA). Subsequently, ^{Dy647}IFNα2 was injected (IFN). (b) Association and dissociation of ^{Dy647}IFNα2 to ^{Dy547}IFNAR2-TM reconstituted in PSM as detected by TIRFS (red curve) and fit of a kinetic model (black curve). For comparison, binding of ^{Dy647}IFNα2 to PSM without IFNAR2-TM is shown (blue curve).

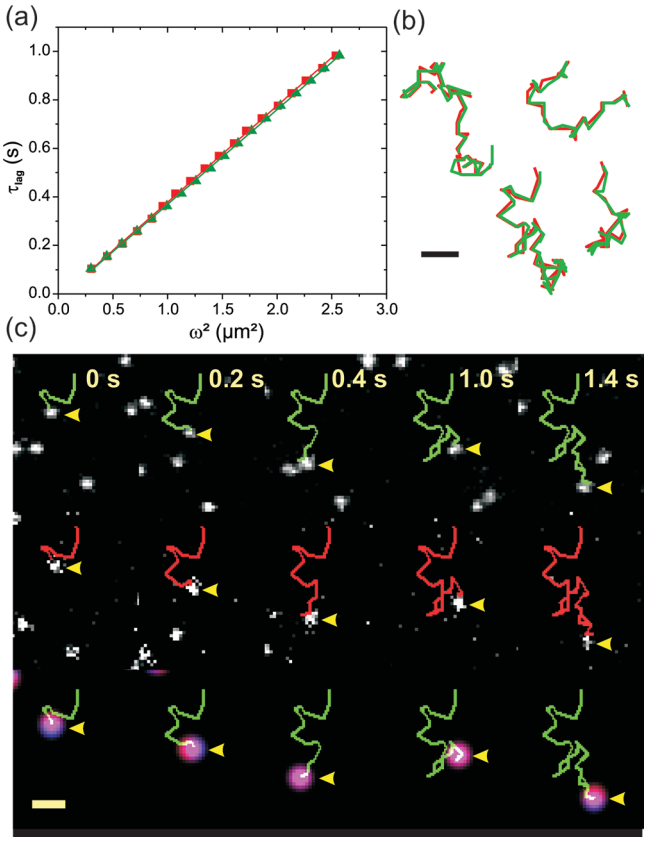

Figure 6. Diffusion and interaction of IFNAR2-TM reconstituted into PSM probed by SMT. (a) Comparison of the mean square displacement (ω^2) for ^{Dy547}IFNAR2-TM reconstituted into PSM and for ^{Dy647}IFNα2 bound to the same membrane. (b) Exemplary trajectories of ^{Dy547}IFNAR2-TM (green) and ^{Dy647}IFNα2 (red) showing colocomotion on the membrane. (c) Time-laps of a diffusing receptor−ligand complex. Single molecule images of ^{Dy547}IFNAR2-TM (top) and ^{Dy647}IFNα2 (center). Colocomotion trajectories were obtained from processed images of colocalized molecules in both channels that are shown in an overlay of ^{Dy547}IFNAR2-TM (blue) and ^{Dy647}IFNα2 (red) (bottom). The scale bars in panels b and c correspond to 1 μm.

constant of 0.74 ± 0.08 $\mu m^2/s$ (Figure 4b,c), similar to the diffusion constant determined by FRAP. Protein diffusion in PSM was also probed by z-scan FCS carried out under the same conditions as the SMT experiments. Typical autocorrelation curves are shown in Figure 4d. From z-scan analysis (Figure 4e,f), a diffusion constant of 2.1 ± 0.4 $\mu m^2/s$ was determined. This value is significantly higher than the diffusion constant observed by FRAP and SMT, suggesting that the very local, submicrometer-scale diffusion is faster compared to diffusion on the scale of several micrometers. However, FCS measurements generally show faster diffusion in membranes compared to FRAP and SMT.[49]

Protein Interactions of IFNAR2-TM Reconstituted into PSM. For probing interactions of membrane protein reconstituted into PSM, we employed the type I interferon receptor subunit IFNAR2, which binds its protein ligand IFNα2 with nanomolar affinity.[50] To this end, transmembrane IFNAR2 without its large, unfolded cytoplasmic domain was expressed in *Sf*9 insect cell, purified from the membrane fraction, and labeled with Dy547 (^{Dy547}IFNAR2-TM). ^{Dy547}IFNAR2-TM was readily reconstituted into VSUV by detergent depletion with cyclodextrin. Simultaneous TIRFS/RIF detection confirmed rapid capturing and fusion of these VSUV to PEG/PA surfaces and efficient incorporation of ^{Dy547}IFNAR2-TM (Figure 5a). After washing off excess lipids by intensive washing at a flow rate of 125 μL/s, 50 nM IFNα2 labeled with Dy647 (^{Dy647}IFNα2) was injected. Fast, reversible binding of ^{Dy647}IFNα2 was observed, while no significant binding could be observed in the

dx.doi.org/10.1021/ac201294v |*Anal. Chem.* 2011, 83, 6792–6799

absence of IFNAR2 (Figure 5b). The binding curve was very well fitted by a 1:1 Langmuir model taking mass transport limitation into account. An association rate constant of $(2.0 \pm 0.5) \times 10^6$ M^{-1} s^{-1} and a dissociation rate constant of (0.033 ± 0.005) s^{-1} were obtained from the fit, which are in very good agreement with the rate constants observed for the interaction of fluorescent labeled IFNα2 with the ectodomain of IFNAR2.[51,52]

For probing protein−protein interactions in PSM on the single molecule level, ^{Dy547}IFNAR2-TM was reconstituted into VSUV and fused on the surface at low concentrations. Free diffusion of ^{Dy547}IFNAR2-TM was confirmed by SMT (Video 3 in the Supporting Information and Figure 6a) and by FCS (Figure S-7 in the Supporting Information). Specific interaction of ^{Dy647}IFNα2 with ^{Dy547}IFNAR2-TM reconstituted into PSM was also detectable by single molecule imaging. To this end, we probed the diffusion of ^{Dy647}IFNα2 interacting with ^{Dy547}IFNAR2-TM in the membrane. Analysis of trajectories obtained for ^{Dy547}IFNAR2-TM and for ^{Dy647}IFNα2 (Figure 6a) yielded an identical diffusion constant (0.64 and 0.63 $\mu m^2/s$, respectively), which were in good agreement with the diffusion constant observed for MBP-TM1. Upon simultaneous dual-color single molecule imaging, colocomotion of individual ^{Dy647}IFNα/^{Dy547}IFNAR2-TM complexes could be clearly discerned (Video 4 in the Supporting Information and Figure 6b,c) despite relatively fast photobleaching of Dy647 (Figure S-8 in the Supporting Information). Thus, specific protein binding to a reconstituted transmembrane receptor was confirmed on the single molecule level.

CONCLUSIONS

We have here established a versatile analytical platform for probing diffusion and interactions of reconstituted membrane proteins in polymer-supported membranes. This approach involves reconstitution of transmembrane proteins into VSUV by detergent extraction with cyclodextrin. This method is compatible with a broad spectrum of detergents used for membrane protein solubilization[39,53] and allows for rapid and automatized membrane protein reconstitution.[53] In contrast to classic heterogeneous phase reconstitution techniques using polymer beads for detergent adsorption,[54] these proteoliposomes can be immediately applied for assembly of PSM. Highly specific capturing of VSUV to a dense PEG polymer brush functionalized with palmitic acid groups was achieved, which is much faster compared to spontaneous fusion on cellulose support.[45] Fusion of captured vesicle and assembly of the membrane are induced by PEG solution, thus giving the opportunity to mix vesicles containing different components on demand. Moreover, the surface can be regenerated with detergent solution and therefore the same substrate can be used repeatedly. This is particularly useful in combination with automated microfluidics, providing the possibility for rapid assays with minimum sample consumption. Thus, membrane composition and protein concentrations can be readily varied. We have demonstrated that diverse spectroscopic techniques are compatible with these PSM. Label-free solid phase detection as well as TIRFS detection in a flow-through format could be used for probing vesicle binding and fusion as well as interactions with a reconstituted membrane protein. Moreover, lipid and protein diffusion was characterized in detail by fluorescence correlation spectroscopy and single molecule imaging. These techniques not only confirmed homogeneous membranes on the micro- to submicrometer scale but also allow exploring protein function and dynamics on the single molecule level. Thus, it was possible to track individual protein complexes in PSM. The simple, rapid, and rugged PSM format presented here is particularly useful for such functional studies on reconstituted membrane proteins, because incubation with different samples is readily achieved by microfluidic sample handling. This analytical platform is well suitable for functional analysis of membrane proteins in a defined lipid environment, requiring minute protein quantities and offering very rapid reconstitution schemes, which are readily automatized. These features are particularly important for membrane proteins, which are often very fragile and difficult to obtain in large quantities. The versatile bottom-up surface chemistry is compatible with all glass-type substrates, offering broad application of spectroscopic and microscopic techniques. Moreover, patterning of the membrane can be readily achieved by photodeprotection strategies as demonstrated before for protein immobilization,[52] which will allow multiplexed assay formats.

ASSOCIATED CONTENT

Supporting Information. Additional information as noted in text. This material is available free of charge via the Internet at http://pubs.acs.org.

AUTHOR INFORMATION

Corresponding Author

*Address: Division of Biophysics, Barbarastrasse 11, 49076 Osnabrück, Germany. E-mail: piehler@uos.de.

ACKNOWLEDGMENT

We thank Gabriele Hikade and Hella Kenneweg for technical support, Jörg Nordmann and Markus Haase for the help with the dynamic light scattering, and Götz Hofhaus for transmission electron microscopy. This project was supported by funding from the DFG (Grants PI405-4, PI405-5, and SFB 944) and by the European Community's Seventh Framework Programme (FP7/2007-2013) under Grant Agreement No. 223608 (IFNaction). J.P was supported by a Heisenberg Professorship from the DFG (Grant PI405-3). S.W. was supported by a FP6Marie-Curie EST fellowship (Grant No. MEST-CT-2004-504272) and by a Ph.D. fellowship from the Minerva Foundation.

REFERENCES

(1) Stubbs, C. D.; Smith, A. D. *Biochim. Biophys. Acta: Rev. Biomembr.* **1984**, *779*, 89.
(2) Lee, A. G. *Biochim. Biophys. Acta* **2004**, *1666*, 62.
(3) Jensen, M. O.; Mouritsen, O. G. *Biochim. Biophys. Acta* **2004**, *1666*, 205.
(4) Andersen, O. S.; Koeppe, R. E., 2nd. *Annu. Rev. Biophys. Biomol. Struct.* **2007**, *36*, 107.
(5) Phillips, R.; Ursell, T.; Wiggins, P.; Sens, P. *Nature* **2009**, *459*, 379.
(6) Rickman, C.; Medine, C. N.; Dun, A. R.; Moulton, D. J.; Mandula, O.; Halemani, N. D.; Rizzoli, S. O.; Chamberlain, L. H.; Duncan, R. R. J *Biol. Chem.* **2010**, *285*, 13535.
(7) Diez, M.; Zimmermann, B.; Borsch, M.; Konig, M.; Schweinberger, E.; Steigmiller, S.; Reuter, R.; Felekyan, S.; Kudryavtsev, V.; Seidel, C. A.; Graber, P. *Nat. Struct. Mol. Biol.* **2004**, *11*, 135.
(8) Margittai, M.; Widengren, J.; Schweinberger, E.; Schroder, G. F.; Felekyan, S.; Haustein, E.; Konig, M.; Fasshauer, D.; Grubmuller, H.; Jahn, R.; Seidel, C. A. *Proc. Natl. Acad. Sci. U.S.A.* **2003**, *100*, 15516.

(9) Lu, H. P. *Curr. Pharm. Biotechnol.* **2009**, *10*, 522.
(10) Garcia-Saez, A. J.; Schwille, P. *Biochim. Biophys. Acta* **2010**, *1798*, 766.
(11) Hern, J. A.; Baig, A. H.; Mashanov, G. I.; Birdsall, B.; Corrie, J. E.; Lazareno, S.; Molloy, J. E.; Birdsall, N. J. *Proc. Natl. Acad. Sci. U.S.A.* **2010**, *107*, 2693.
(12) Heyse, S.; Stora, T.; Schmid, E.; Lakey, J. H.; Vogel, H. *Biochim. Biophys. Acta: Rev. Biomembr.* **1998**, *1376*, 319.
(13) Janshoff, A.; Steinem, C. *ChemBioChem* **2001**, *2*, 798.
(14) Cooper, M. A. *J. Mol. Recognit.* **2004**, *17*, 286.
(15) Kiessling, V.; Crane, J. M.; Tamm, L. K. *Biophys. J.* **2006**, *91*, 3313.
(16) Fox, C. B.; Wayment, J. R.; Myers, G. A.; Endicott, S. K.; Harris, J. M. *Anal. Chem.* **2009**, *81*, 5130.
(17) Thompson, N. L.; Wang, X.; Navaratnarajah, P. *J. Struct. Biol.* **2009**, *168*, 95.
(18) Kelety, B.; Diekert, K.; Tobien, J.; Watzke, N.; Dorner, W.; Obrdlik, P.; Fendler, K. *Assay Drug Dev. Technol.* **2006**, *4*, 575.
(19) Jung, H.; Robison, A. D.; Cremer, P. S. *J. Struct. Biol.* **2009**, *168*, 90.
(20) Tanaka, M.; Sackmann, E. *Nature* **2005**, *437*, 656.
(21) Sackmann, E.; Tanaka, M. *Trends Biotechnol.* **2000**, *18*, 58.
(22) Tanaka, M.; Tutus, M.; Kaufmann, S.; Rossetti, F. F.; Schneck, E.; Weiss, I. M. *J. Struct. Biol.* **2009**, *168*, 137.
(23) Janshoff, A.; Steinem, C. *Anal. Bioanal. Chem.* **2006**, *385*, 433.
(24) Heyse, S.; Ernst, O. P.; Dienes, Z.; Hofmann, K. P.; Vogel, H. *Biochemistry* **1998**, *37*, 507.
(25) Wagner, M. L.; Tamm, L. K. *Biophys. J.* **2000**, *79*, 1400.
(26) Wagner, M. L.; Tamm, L. K. *Biophys. J.* **2001**, *81*, 266.
(27) Ataka, K.; Giess, F.; Knoll, W.; Naumann, R.; Haber-Pohlmeier, S.; Richter, B.; Heberle, J. *J. Am. Chem. Soc.* **2004**, *126*, 16199.
(28) Sinner, E. K.; Ritz, S.; Naumann, R.; Schiller, S.; Knoll, W. *Adv. Clin. Chem.* **2009**, *49*, 159.
(29) Li, E.; Merzlyakov, M.; Lin, J.; Searson, P.; Hristova, K. *J. Struct. Biol.* **2009**, *168*, 53.
(30) Sigl, H.; Brink, G.; Seufert, M.; Schulz, M.; Wegner, G.; Sackmann, E. *Eur. Biophys. J.: Biophys. Lett.* **1997**, *25*, 249.
(31) Knoll, W.; Frank, C. W.; Heibel, C.; Naumann, R.; Offenhausser, A.; Ruhe, J.; Schmidt, E. K.; Shen, W. W.; Sinner, A. *J. Biotechnol.* **2000**, *74*, 137.
(32) Kalb, E.; Frey, S.; Tamm, L. K. *Biochim. Biophys. Acta* **1992**, *1103*, 307.
(33) Deverall, M. A.; Gindl, E.; Sinner, E. K.; Besir, H.; Ruehe, J.; Saxton, M. J.; Naumann, C. A. *Biophys. J.* **2005**, *88*, 1875.
(34) Ye, Q.; Konradi, R.; Textor, M.; Reimhult, E. *Langmuir* **2009**, *25*, 13534.
(35) Deng, Y.; Wang, Y.; Holtz, B.; Li, J.; Traaseth, N.; Veglia, G.; Stottrup, B. J.; Elde, R.; Pei, D.; Guo, A.; Zhu, X. Y. *J. Am. Chem. Soc.* **2008**, *130*, 6267.
(36) Groves, J. T.; Boxer, S. G. *Acc. Chem. Res.* **2002**, *35*, 149.
(37) Oliver, A. E.; Parikh, A. N. *Biochim. Biophys. Acta* **2010**, *1798*, 839.
(38) Cooper, M. A.; Hansson, A.; Lofas, S.; Williams, D. H. *Anal. Biochem.* **2000**, *277*, 196.
(39) Degrip, W. J.; Vanoostrum, J.; Bovee-Geurts, P. H. *Biochem. J.* **1998**, *330* (Pt 2), 667.
(40) Piehler, J.; Brecht, A.; Valiokas, R.; Liedberg, B.; Gauglitz, G. *Biosens. Bioelectron.* **2000**, *15*, 473.
(41) Gavutis, M.; Lata, S.; Lamken, P.; Muller, P.; Piehler, J. *Biophys. J.* **2005**, *88*, 4289.
(42) Gavutis, M.; Lata, S.; Piehler, J. *Nat. Protoc.* **2006**, *1*, 2091.
(43) Signorell, G. A.; Kaufmann, T. C.; Kukulski, W.; Engel, A.; Remigy, H. W. *J. Struct. Biol.* **2007**, *157*, 321.
(44) Lentz, B. R. *Eur. Biophys. J.* **2007**, *36*, 315.
(45) Goennenwein, S.; Tanaka, M.; Hu, B.; Moroder, L.; Sackmann, E. *Biophys. J.* **2003**, *85*, 646.
(46) Humpolickova, J.; Gielen, E.; Benda, A.; Fagulova, V.; Vercammen, J.; Vandeven, M.; Hof, M.; Ameloot, M.; Engelborghs, Y. *Biophys. J.* **2006**, *91*, L23.
(47) Benda, A.; Beneš, M.; Mareček, V.; Lhotský, A.; Hermens, W. T.; Hof, M. *Langmuir* **2003**, *19*, 4120.
(48) Przybylo, M.; Sykora, J.; Humpolickova, J.; Benda, A.; Zan, A.; Hof, M. *Langmuir* **2006**, *22*, 9096.
(49) Guo, L.; Har, J. Y.; Sankaran, J.; Hong, Y.; Kannan, B.; Wohland, T. *ChemPhysChem* **2008**, *9*, 721.
(50) Piehler, J.; Schreiber, G. *J. Mol. Biol.* **1999**, *289*, 57.
(51) Lata, S.; Gavutis, M.; Piehler, J. *J. Am. Chem. Soc.* **2006**, *128*, 6.
(52) Waichman, S.; Bhagawati, M.; Podoplelova, Y.; Reichel, A.; Brunk, A.; Paterok, D.; Piehler, J. *Anal. Chem.* **2010**, *82*, 1478.
(53) Iacovache, I.; Biasini, M.; Kowal, J.; Kukulski, W.; Chami, M.; van der Goot, F. G.; Engel, A.; Remigy, H. W. *J. Struct. Biol.* **2010**, *169*, 370.
(54) Rigaud, J. L.; Mosser, G.; Lacapere, J. J.; Olofsson, A.; Levy, D.; Ranck, J. L. *J. Struct. Biol.* **1997**, *118*, 226.